Quantum calculation of intramultiplet mixing: Comparison with simple radial and angular mechanisms

Roger W. Anderson

Citation: The Journal of Chemical Physics **77**, 5426 (1982); doi: 10.1063/1.443792
View online: http://dx.doi.org/10.1063/1.443792
View Table of Contents: http://scitation.aip.org/content/aip/journal/jcp/77/11?ver=pdfcov
Published by the AIP Publishing

Quantum calculation of intramultiplet mixing: Comparison with simple radial and angular mechanisms

Roger W. Anderson

Chemistry Board of Studies, University of California, Santa Cruz, Calfornia 95064
(Received 13 November 1981; accepted 24 December 1981)

Cross sections for intramultiplet mixing in the lowest ^2P states of alkali atoms (K, Rb, Cs) in collisions with He atoms are calculated in body fixed coordinates. The cross sections for transitions that maintain or change the magnitude of the projection of the electronic angular momentum are compared with very simple semiclassical models for radial (R_1) and angular (R_2) coupling of electronic states. The angular mixing model uses a hard sphere interaction. The agreement is good for the total cross sections and for the transition probabilities for different partial waves. The total cross sections are compared with experimental and other theoretical results, and cross sections are presented for collisions of polarized $^2P_{3/2}$ atoms. The quantum mechanical equations are integrated with a constant step size Magnus method, and we find uniform convergence $O(h^2)$ for small step sizes. The error rapidly increases for steps large enough to allow propagation of a channel by half of a de Broglie wavelength.

I. INTRODUCTION

During the past 15 years there has been much theoretical and experimental interest in intramultiplet mixing in excited alkali atom collisions with noble gas atoms and molecules. The experiments were first performed by Wood[1] more than 65 years ago, and many thermal average cross sections were obtained much later in the 1960s by Krause.[2] Early theoretical work was done by Nikitin[3] and Callaway and Bauer[4] who used semiclassical collision theory with exchange[3] or van der Waals[4] interactions. Nikitin[5] and co-workers[6,7] have made numerous additional contributions over later years, and the main significance of this work is that two mechanisms—radial and angular or Coriolis—are responsible for intramultiplet mixing. Reid and Dalgarno[8,9] did the first quantum mechanical calculations of the intramultiplet transitions in Na($3p$) collisions with He. In addition to describing how to do the quantum calculations, they also established the importance of exchange interactions in causing intramultiplet transitions.

This theoretical activity inspired experiments to measure the velocity dependence of intramultiplet mixing. Gallagher[10] measured the temperature dependence of Rb($5p$) and Cs($6p$) intramultiplet mixing, and he deduced $Q(v)$ for the systems. Anderson, Goddard, Parravano, and Warner[11] performed the first crossed molecular beam determination of $Q(v)$ for mixing in K($4p$) collisions with He. Cuvellier *et al.*[12] have repeated and extended these measurements. Mestdagh *et al.*[13] have recently also measured $Q(v)$ for K($4p$) transitions in N_2 and Ar collisions. Phillips, Glaser, and Kleppner[14] have used crossed beams with doppler velocity selection to measure $Q(v)$ for Na($3p$) mixing in Ne, Ar, and Kr collisions. Phillips *et al.*[15] have studied angular distributions by means of doppler spectroscopy. Apt and Pritchard[16] have determined $Q(v)$ for Na($3p$) transitions in a gas cell by using doppler velocity selection.

While the experiments have been done, others have been active in doing quantum calculations. Olson[17] and Pascale and Olson[18] have used the potentials of Baylis[19] to calculate a variety of cross sections and thermal averages. Wilson and Shimoni[20] have done quantum calculations. Recently, Pascale and Perrin[21] have calculated cross sections for polarized K($^2P_{3/2}$) atoms. Much recent work has been devoted to semiclassical[7,22] and even classical[23] approaches.

In this paper our main goal is to compare accurate quantum mechanical calculations with simple models for radial and angular coupling. The interatomic separations important for the two forms of coupling are indicated in Fig. 1. The radial coupling occurs at relatively large distances at R_1. At this radius the exchange interaction that provides the splitting between the $^2\Sigma_{1/2}$ and $^2\Pi_{1/2}$ states is large enough to cause a change in the coupling from the long range Hund's (c) case. Radial motion in this region can cause intramultiplet mixing that conserves Ω. Angular coupling tends to occur at interatomic separations R_2 near the classical turning point on the Π states. When the atoms are close together, the interatomic axis can rotate most rapidly and cause mixing of the $^2\Pi_{1/2}$ and $^2\Pi_{3/2}$ states. The angular mechanism changes Ω by ± 1. Nikitin[5,6] has discussed these mechanisms in detail.

In Sec. II we review the quantum formulation of the

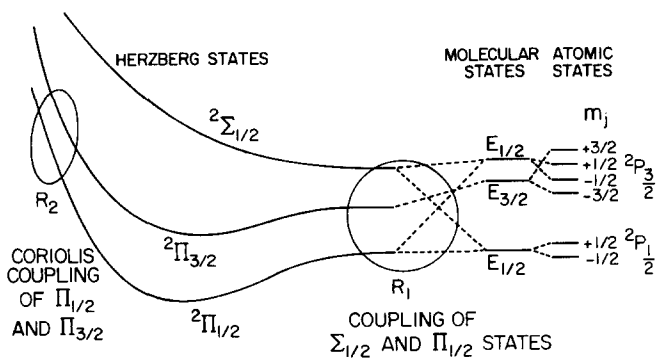

FIG. 1. Schematic representation of the interactions of the diatomic states arsing from a ^2P alkali atom and a noble gas atom. The R_1 radial coupling, and R_2 angular or Coriolis coupling regions are shown.

 021-9606/82/235426-10$02.10

intramultiplet mixing problem, and we discuss how the usual space fixed axis T^J matrices can be easily transformed into T^J matrices appropriate for body fixed axes. It is only reasonable to discuss processes that maintain or change Ω in body fixed axes.

Section III outlines the numerical procedure that we use to integrate the coupled equations that describe intramultiplet mixing. The convergence of the method and an instability that occurs for large steps is described.

Section IV contains a description of a very simple radial coupling model. We assume the probability expression first obtained by Nikitin,[5] and we discuss the assumptions we make in converting it to a $P(l)$. Section V presents a hard sphere angular mixing mechanism. Angular transitions are described for a potential that treats the alkali and noble gas atoms as hard spheres. Again simple expressions are given for $P(l)$.

The discussion is in Sec. VI. Here the results of our calculations using the alkali-noble gas potentials of Pascale and Van de Planque[24] are compared with other calculations and experiments that determine the velocity dependence of fine structure state changing collisions. The discussion also includes a detailed comparison of the body fixed quantum results and the results of the simple radial and angular mechanisms.

II. QUANTUM THEORY

The quantum mechanical calculations reported here employ the Reid and Dalgarno[8,9] formalism that has also been used by Olson,[17] Pascale and Olson,[18] and most recently by Pascale and Perrin[21] to treat transitions among the lowest np^2P_{jm} states of an alkali atom in collisions with noble-gas atoms. The essence of the formalism is the recognition that the fine structure state transitions are rotational transitions where the angular momentum j and its projection m is changed by the collision to j' and m'. Reid and Dalgarno use the Arthurs and Dalgarno[25] theory for the excitation of a rigid rotor in collision with an atom. The important requirement for rotational transitions is an anisotropic potential, and Reid and Dalgarno use a Legendre polynomial expansion of the interactions of the ^2P electron with the noble gas atom. Two terms are necessary, giving

$$V(\mathbf{r},\mathbf{R}) = V_0(\mathbf{r},\mathbf{R})\,P_0(\mathbf{r}\cdot\mathbf{R}) + V_2(\mathbf{r},\mathbf{R})\,P_2(\mathbf{r}\cdot\mathbf{R}) \ , \qquad (1)$$

where $\mathbf{r}$ is the coordinate of the alkali ^2P electron and $\mathbf{R}$ is the relative coordinate of the alkali and noble gas atoms. The Legendre expansion is well justified at large R if the molecular states of the diatomic system are described by a single np configuration of the alkali atom. At smaller R, where exchange and configuration mixing are important, the two term expansion must be justified semiempirically as a convenient way to account for the interaction. For the calculations in this paper, the potentials of Pascale and Van de Planque[24] (PV) have been used to determine V_0 and V_2. Reid[9] clearly presents the equations that give V_0 and V_2 from adiabatic potentials.

To treat the collision, Reid and Dalgarno[8,9] use eigenfunctions of J^2, J_z, l^2, and j^2, where J is the total angular momentum of the system, J_z is its projection, l is the angular momentum of the relative motion of the atoms, and j is the angular momentum of the alkali valance electron. The angular momenta and coordinates are relative to *space fixed* axes. The coupled equations that result from this basis with the coupling given by Eq. (1) are very clearly described by Reid.[9] We do not repeat them here. We have solved these equations in spaced fixed axes to generate transition matrix elements $\langle jl|\,T^J\,|j'l'\rangle$. The equations are numerically solved by a constant step size Magnus method that is described in Sec. III.

The matrix elements of the T matrix correspond to transitions from a state of $|jl\rangle$ to a state $|j'l'\rangle$, where $j+l=j'+l'=J$. Reid[9] and Pascale and Perrin[21] use these transition matrix elements to give cross sections for transitions $jm\to j'm'$, where m and m' are the projections of j with respect to *space fixed* axes. Since one of our main objectives in this paper is to show the correspondence of the quantum calculations with simple semiclassical models for radial and angular mechanisms, we must transform our transition matrices into *body fixed* axes. This is necessary because radial coupling (R_1 mechanism) will correspond to transitions $j\to j'$ where $|m|=|m'|=\frac{1}{2}$ where m and m' are referred to body fixed axes. The radial coupling conserves the absolute value of the projection of the alkali angular momentum with respect to the final relative velocity of the scattered atoms. Similarly the angular mechanism corresponds to transitions where $|m|=|m'|\pm 1$ with respect to *body fixed* axes.

Fortunately, transition matrix elements in body fixed coordinates are easily found. The body fixed or helicity representation T matrix elements[26,27] are given by

$$\langle jm|\,T^J\,|j'm'\rangle = \sum_{ll'} i^{l-l'}\langle jJm-m|\,jJl0\rangle \times\langle jl|\,T^J\,|\,j'l'\rangle\langle j'Jl'0|\,j'Jm'-m'\rangle \ .$$

In this equation $\langle jJm-m|jJl0\rangle$ and $\langle j'Jl'0|\,j'Jm'-m'\rangle$ are Clebsch–Gordan coefficients[28] and $\langle jl|\,T^J|\,j'l'\rangle$ are the T matrix elements obtained from the space fixed axis calculation. It is important to stress that the projections m and m' now correspond to body fixed axes or a coordinate system that rotates with the diatom system.

In terms of the transition matrix elements $\langle jm|\,T^J|\,j'm'\rangle$, the differential and total cross sections for the $jm\to j'm'$ transitions are[27]

$$\frac{d\sigma(jm;\,j'm')}{d\Omega} = \frac{1}{4k_j^2}\left|\sum_{J=1/2}^{\infty}(2J+1)\langle jm|\,T^J\,|j'm'\rangle \times d^J_{mm'}(\theta)\right|^2$$

and

$$\sigma(jm;\,j'm') = \frac{\pi}{k_j^2}\sum_{J=1/2}^{\infty}(2J+1)\left|\langle jm|\,T^J\,|j'm'\rangle\right|^2 \ .$$

In these equations k_j is the wave number for the state of electronic angular momentum j and $d^J_{mm'}(\theta)$ are ro-

tation matrices.[28] We also note that the total angular momenta J assume half-integral values.

To provide correspondence between the quantum calculations and the radial or angular coupling models, we now consider probabilities and cross sections for $j=\frac{1}{2}\rightarrow j'=\frac{3}{2}$, where for the radial coupling case $|m| = |m'| = \frac{1}{2}$ and for the Coriolis or angular case $|m| = \frac{1}{2}$ and $|m'| = \frac{3}{2}$. The appropriate transition probabilities are calculated as

$$P_{1/2}(J)=\frac{1}{2}\sum_{|m|=1/2,|m'|=1/2}\left|\langle\tfrac{1}{2}m|\,T^J\,|\tfrac{3}{2}m'\rangle\right|^2, \qquad (2a)$$

$$P_{3/2}(j)=\frac{1}{2}\sum_{|m|=1/2,|m'|=3/2}\left|\langle\tfrac{1}{2}m|\,T^J\,|\tfrac{3}{2}m'\rangle\right|^2.$$

The total cross sections for the radial or Coriolis coupling cases are given as

$$Q_{1/2}=\frac{\pi}{k_j^2}\sum_{J=1/2}^{\infty}(2J+1)P_{1/2}(J), \qquad (2b)$$

$$Q_{3/2}=\frac{\pi}{k_j^2}\sum_{J=1/2}^{\infty}(2J+1)P_{3/2}(J),$$

where $j=\frac{1}{2}$. The total cross section for intramultiplet mixing is $Q_{1/2}+Q_{3/2}$ and is clearly the same in space or body fixed axes.

III. CONSTANT STEP SIZE MAGNUS INTEGRATION

The results in this paper are obtained by dividing the range of the integration into N equal size intervals of length h. In the middle of each interval the potential plus centrifugal energy matrix is diagonalized and the wave function at the small R side of the interval is transformed into the diagonalized basis. The eigenvalues are used to construct Magnus propagators.[29] These propagators give the evolution of the quasiadiabatic wave function over the interval. At the large R side of the interval the wave function is again transformed into the original basis and the next interval is treated in the same way. A detailed account of the method that is based on Light's original formulation is given by Anderson.[30]

Care is taken in the calculations to start the integrations at a suitable R_s, where the evolution of the wave functions at still smaller R can be neglected in establishing the asymptotic form of the wave functions. For all calculations in this paper, R_s is $3.5a_0$. The asymptotic form of the wave functions at large R are expanded in Ricatti–Bessel functions to calculate the R matrix[31] for each value of J. The S matrix is then obtained[31] and the T matrix elements are easily found. For these calculations the scattering matrices were evaluated after integrating the equations to $R=30a_0$.

We use the constant step size Magnus method because, in previous work by Mitchell and Anderson[32] and Anderson,[30] it is shown that the method converges with a small number of intervals and the convergence of the method is monotonic and uniform, provided that no channel is propagated by more than one-half of its local de Broglie wavelength. For step sizes greater than one-half, a de Broglie wavelength, the error in the method increases very rapidly. Mitchell and Anderson call this abrupt increase in the error the "magic π," and they give a perturbation theory analysis. The practical importance of the magic π effect is that the step size for a calculation, which is to be done for several energies, is determined by the de Broglie wavelength for the highest energy calculation. For the results presented here, the maximum energy is typically 2500 Kayser (1 Kayser = 1 cm^{-1}). If convergence is obtained with N intervals for this energy, the calculation will certainly be good for lower energies.

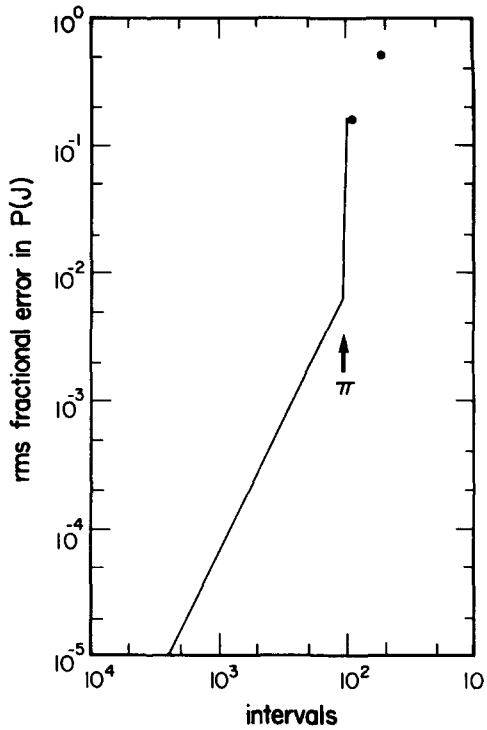

FIG. 2. The rms fractional errors in $P(J)$ as a function of the number of intervals. The arrow indicates the number of intervals that give $kh=\pi$.

Figure 2 presents the rms fractional error of $P(J)$ for a Rb+He calculation at $E=2500$ K as a function of the number of integration intervals. $P(J)$ for this figure is the probability for a total angular momentum J of an inelastic collision that has $|m| = |m'|$ in body fixed axes $[P_{1/2}(J)]$. We note that for $N>107$ intervals, the convergence is monotonic $O(h^2)$, but that the error rapidly increases for smaller numbers of intervals. The arrow in the figure marks the number of intervals where $kh=\pi$. We see that a calculation with 212 intervals ($h=0.125a_0$) has a rms fractional error of only 0.15% for $E=2500$. We use this step size for all calculations in this work. The rms fractional error for $P_{3/2}(J)$ is almost identical for $N>107$. In the large error region both $P_{1/2}(J)$ and $P_{3/2}(J)$ exhibit the magic π instability, but the errors differ by as much as a factor of 2 for the two probabilities.

The total cross section results of this work are shown in Figs. 3 and 4. The radial or angular cross sections for $^2P_{3/2}\rightarrow{}^2P_{1/2}$ transitions are easily obtained from the $Q_{1/2}$ and $Q_{3/2}$ defined by Eqs. (2b) by detailed balance. Figure 5 shows the $^2P_{3/2}\rightarrow{}^2P_{1/2}$ cross sections for K

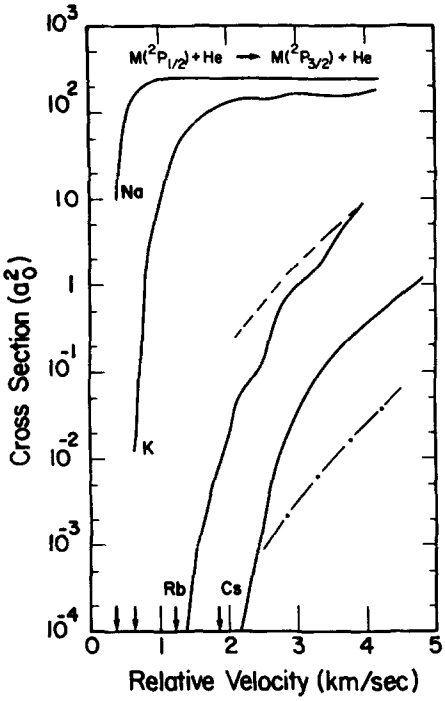

FIG. 3. Total cross sections for $^2P_{1/2}$ to $^2P_{3/2}$ transitions for alkali atoms in collisions with He. The solid lines are from the CC calculations of this paper. The dashed line is Gallagher's results for Rb+He and the dot–dash line is his result for Cs+He. The arrows at the bottom of the figure indicate the minimum relative velocity necessary to provide the endoergicity of the process for the four systems.

+He. Figure 6 presents the results of this work for $Q_{1/2}$ and $Q_{3/2}$ for K, Rb, and Cs+He.

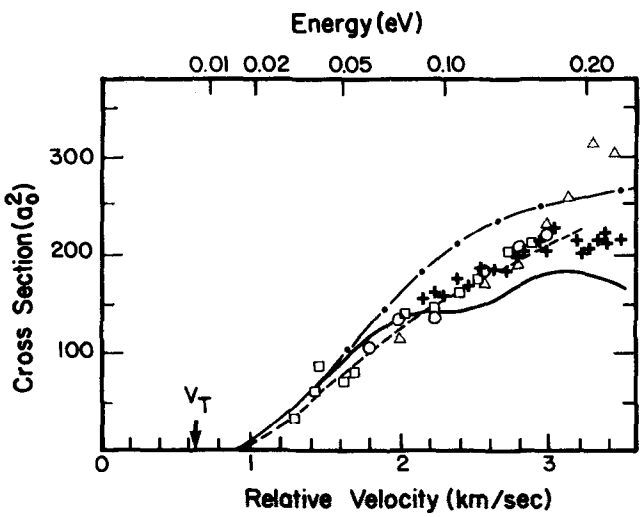

FIG. 4. Total cross sections for $K(4p\,^2P_{1/2})+He \rightarrow K(4p\,^2P_{3/2})+He$. The solid line is the result of this work. The dot–dash line is the calculation of Roueff and Launay, and the dashed line is the semiclassical result of Anderson *et al.* The circles and squares are experimental results of Anderson *et al.* and the crosses are experimental results of Cuvellier *et al.* The experimental results are normalized together and to the semiclassical result of Anderson *et al.*

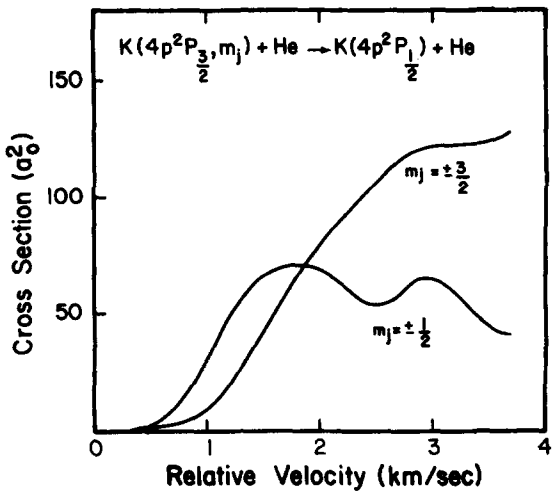

FIG. 5. Dependence of $K(4p\,^2P_{3/2}) \rightarrow K(4p\,^2P_{1/2})$ cross sections on the m_j sublevels of the $^2P_{3/2}$ state.

IV. NIKITIN R_1 (RADIAL) MECHANISM

By solving the two state problem with classical motion of the atoms, constant spin-orbit interaction, and an exponential $\Sigma-\Pi$ splitting, Nikitin[5] gives for the probability of a $^2\Pi_{1/2}$ to $^2\Sigma_{1/2}$ transition

$$P_1\left(\frac{v_R}{v_N}\right) = 2\exp(-v_N/3v_R)\sinh(2v_N/3v_R) \times \sinh(v_N/3v_R)/\sinh^2(v_N/v_R)\,, \qquad (3)$$

where v_R is the radial velocity at R_1 and $v_N \equiv \pi\Delta\epsilon/\hbar\alpha$.

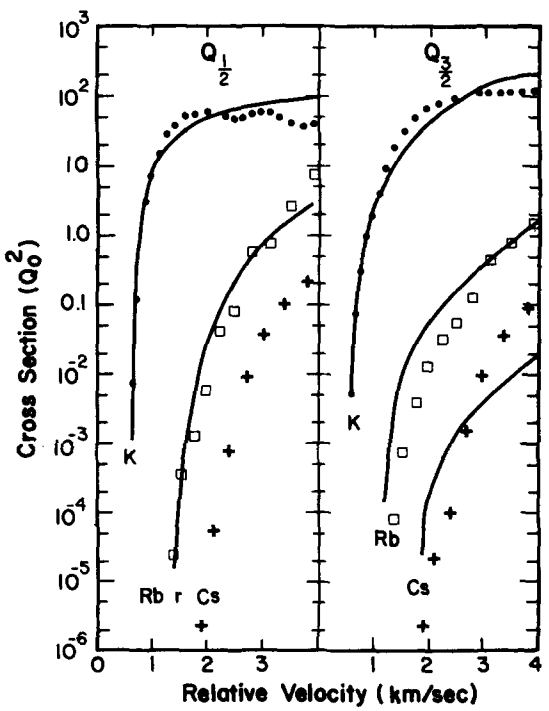

FIG. 6. Comparison of the radial $Q_{1/2}$ and Coriolis $Q_{3/2}$ cross sections of the CC calculations with the results of the simple radial and Coriolis models. The CC results for K+He are solid circles, Rb+He are squares, and Cs+He are crosses. The simple model results are the solid lines.

TABLE I. Parameters for semiclassical model calculations.

System	ΔE (Kayser)	Radial model $R_1(a_0)$	Radial model $\alpha(a_0^{-1})$	Angular model $\sigma(a_0)$	Angular model ω(Kayser)
K+He	57.72	10.5	0.89	5	40
Rb+He	237.6	8	0.70	6	180
Cs+He	554.04	...	...	6	505

$\Delta\epsilon$ is the fine structure splitting for the isolated atom and α determines the $\Sigma-\Pi$ interaction by

$$V(\Sigma) - V(\Pi) = A \exp(-\alpha R) .$$

Nikitin argues that α is given by $2\sqrt{2I^*}$, where I^* is the ionization potential of the excited alkali atom in atomic units. This choice is consistent with the PV potential for K+He, but $\alpha = 0.7$ as given in Table I is a better value for Rb($5p^2P$).

The expression for the probability can be simplified with the substitution $y = \exp(-2v_N/3v_R)$. Then

$$P_1(v_R/v_N) = 2y^2(1+y)/(1+y+y^2)^2 .$$

When v_R is very much less than v_N

$$P_1(v_R/v_N) \sim 2\exp(-4v_N/3v_R) .$$

When v_R is much larger than v_N, $y \approx 1$, and $P_1(v_R/v_N) \sim 4/9$. At thermal energies, the alkali atom–helium systems (where the alkali is in its lowest ^2P state) have a wide range for that ratio v_R/v_N. For sodium $v_R/v_N \gg 1$, and for rubidium $v_R/v_N \ll 1$.

For classical motion of the nuclei

$$v_R = v\sqrt{(b_m^2 - b^2)/R_1^2} ,$$

where the velocity v is determined by the initial kinetic energy and b_m is the maximum impact parameter that allows approach of the diatom system to R_1. R_1 is the radius at which $V(\Sigma) - V(\Pi) = \Delta\epsilon$. This b_m is easily determined for motion of the atoms on a single potential. However, for the two state problem an effective potential must be used for the trajectory that accounts for motion on both potentials. This is a problem with any semiclassical treatment of an excitation problem. If the initial kinetic energy is much greater than the potential at R_1 for either state, the potential for either state may be used in computing the value of v_R at R_1. However, for excitation near threshold, some care must be exercised in choosing v_R in $P(v_R/v_N)$.

Two choices for "v_R" are commonly used in the literature: (1) The arithmetic mean of v_R computed for the two adiabatic potentials. (2) The geometric mean of v_R for the two potentials. Both choices are equivalent for large kinetic energies, but we choose the geometric mean because for that choice v_R approaches zero at threshold.

We now cast the expression for $P(v_R/v_N)$ in terms of the orbital angular momentum quantum number l in order to directly compare the simple semiclassical P with our close coupled results for $P_{1/2}$. We use $v_R = (\dot{R}_i\dot{R}_j)^{1/2}$, where

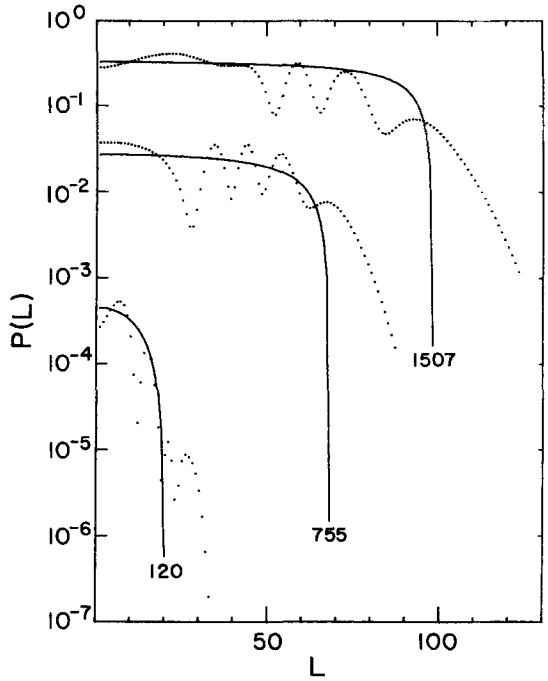

FIG. 7. $P(l)$ for the R_1 mechanism for K+He. The solid lines are the simple model results at the indicated collision energies in Kaysers (1 Kayser = 1 cm^{-1}). The dots are the CC results for $L = J - 1/2$. For clarity the 1507 K results are multiplied by 1.0, the 755 K results by 0.1, and the 120 K results by 0.01.

$$\tfrac{1}{2}\mu\dot{R}_j^2 = E - U_j - \hbar^2 l(l+1)/2\mu R_1^2 .$$

Hence, $\dot{R}_j^2 = v_j^2(1 - l(l+1)/k_j^2 R_1^2)$, where j represents the initial or final adiabatic state, and $v_j^2 = 2E_j/\mu$, $E_j = E - U_j$, and $k_j^2 = 2\mu E_j/\hbar^2$.

Finally, substitution gives

$$v_R(l) = v_i\{[k_i^2 R_1^2 - l(l+1)][k_f^2 R_1^2 - l(l+1)]\}^{1/4}/k_i R_1 . \quad (4)$$

For large values for l, $l_{max} \simeq k_f R_1$. We hence can calculate $P_1(l) = P[v_R(l)/v_N]$. The total cross section for the transition is given by

$$Q_1 = \frac{\pi}{k_i^2}\sum_{l=0}^{l_{max}}(2l+1)P_1(l) \simeq \frac{2\pi}{k_i^2}\sum_{l=0}^{l_{max}} lP_1(l) . \quad (5)$$

Comparison of the Nikitin R_1 mechanism with the close coupled results are given in Figs. 6, 7, and 8 for K–He and Rb–He. The values for R_1 and α are given in Table I. We see an excellent agreement with the magnitude of P_l and Q_1 for Rb and the low velocity K–He systems. We have not presented R_1 results for Cs+He because there is no R for which $V(\Sigma) - V(\Pi) = \Delta\epsilon$ for the PV potentials for this system. The semiclassical result should be good if the transition amplitude for the $^2\Pi_{3/2}$ state is small throughout the collision. This condition is not satisfied for the Na–He system, and for this reason we do not present $Q_{1/2}$ or $Q_{3/2}$ comparisons for Na–He.

V. HARD SPHERE R_2 (CORIOLIS) MECHANISM

Dashevskaya, Nikitin, and Reznikov[8] consider the R_2 mechanism. They write the semiclassical probability

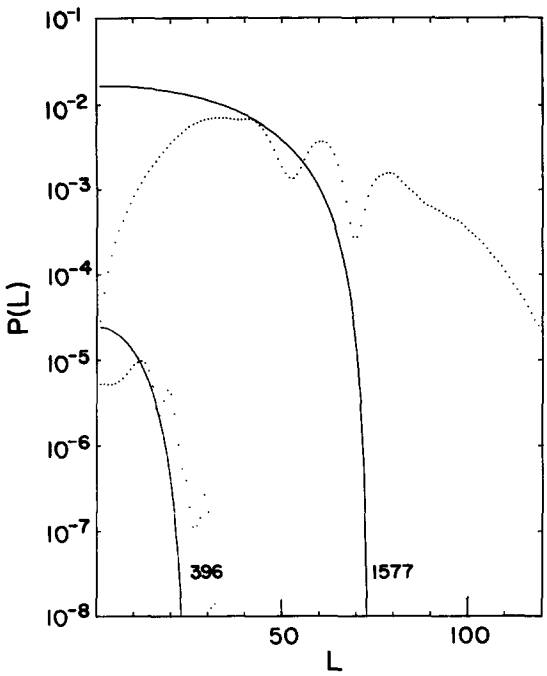

FIG. 8. As Fig. 7 but for Rb+He. The 1577 and 396 K results are multiplied by 1.0.

obtained by adiabatic perturbation theory for this process as

$$P_2(b) = \frac{v^2 b^2}{4} \left| \int_{-\infty}^{\infty} \frac{\exp(i\omega t)\, dt}{R^2(t)} \right|^2 , \tag{6}$$

where ω is the splitting between the $^2\Pi_{1/2}$ and $^2\Pi_{3/2}$ states and $R(t)$ is the time dependent distance between the two atoms. They give ω as $2\Delta\epsilon/3$ and, this value is close to the splitting, we can derive from the potentials of Pascale and Van de Planque for K+He. We use the ω determined from the potentials for Rb+He and Cs +He.

Dashevskaya *et al.*[6] consider the potentials for the $^2\Pi_{1/2}$ and $^2\Pi_{3/2}$ states to be shifted exponentials. They make use of the effective wave number approximation and they obtain a somewhat cumbersome method to evaluate $P_2(b)$ in terms of a function $F(y)$, which they present in a graph. The transition probabilities that they obtain appear reasonable, although this author's evaluation of their integral representation for $F(y)$ differs strongly with their graph.

The exponential potentials give a simple expression for $R(t)$, but the evaluation of $P_2(b)$ is not simple, and no illuminating analytic expressions have been found for this model. We have instead noted their observation that the main part of the transition probability comes from the part of the trajectory close to the turning point. The simplest turning point problem is a hard sphere potential. If the turning point is reached at $t=0$ then

$$R_2(t) = v^2 t^2 + b^2 , \quad b \geq \sigma ,$$

$$R_2(t) = v^2 t^2 + 2vt(\sigma^2 - b^2)^{1/2} + \sigma^2 , \quad b < \sigma .$$

Now we assume that $R(t) = R(-t)$, so

$$P_2(b) = v^2 b^2 \left| \int_0^{\infty} \frac{\cos \omega t\, dt}{R^2(t)} \right|^2 .$$

For $b \geq \sigma$, the integral may be easily evaluated to give

$$P_2(b) = (\pi^2/4) \exp(-2\omega b/v) .$$

The integral for $b < \sigma$ is more difficult. Evaluation of the cosine Fourier integral[33] with the appropriate $R(t)$ yields simple results only for $b = \sigma$. Numerical integration for other values of b is unsatisfactory because the integrand oscillates with a slowly damped amplitude. Numerical integration is however easily accomplished with an exponentially damped integrand. To convert the imaginary exponent in Eq. (6) to a real negative exponent we write

$$P_2(b) = \frac{b^2}{\sigma^2} \left| \mathrm{Re} \int_0^{\infty} \frac{\exp(i\xi t)\, dt}{t^2 + 2at + 1} \right|^2 ,$$

where $a = (1 - b^{*2})^{1/2}$, $b^* = b/\sigma$, and $\xi = \omega\sigma/v$. Now the poles in the integrand occur for $\mathrm{Re}(t) < 0$, for $b^* < 1$. Hence, a contour around the first quadrant will encircle or cross no poles of the integrand. Integration around the contour gives then for $b^* < 1$

$$P_2(b^*) = 4b^{*2}(1 - b^{*2}) \left| \int_0^{\infty} \frac{t \exp(-\xi t)\, dt}{(1 + t^2)^2 - 4b^{*2} t^2} \right|^2 .$$

A simple change of variables gives the useful form

$$P_2(b^*) = 4\xi^{-4} b^{*2}(1 - b^{*2}) \left| \int_0^{\infty} \frac{x \exp(-x)\, dx}{(1 + x^2/\xi^2)^2 - 4b^{*2} x^2/\xi^2} \right|^2 .$$

For $b^* = 0$, the integral can be evaluated in terms of sine and cosine integrals. For large ξ, it is easy to obtain

$$P_2(b^*) = 4b^{*2}(1 - b^{*2})\xi^{-4} .$$

Here we find the interesting result that $P_2(b^*)$ for large ξ is essentially an inverse power of $\Delta\epsilon$. This is a possibly significant result considering the recent success of power law scaling for rotational excitation cross sections.[34]

Semiclassical cross sections may be obtained as

$$Q_2 = \int_0^{\infty} P_2(b)\, d(\pi b^2) = Q_{b<\sigma} + Q_{b>\sigma} .$$

For large ξ, $Q_2 \sim Q_{b<\sigma} \sim 2\pi\sigma/3\xi^4$. We see that the cross section also scales as a power law.

We wish to express P_2 as a function of l and an effective velocity in order to compare with the close coupled calculation. We use $v = (v_i v_f)^{1/2}$ in the calculation of ξ. Then with $k = (k_i k_f)^{1/2}$, $l_c = k\sigma$, $l = kb$, and $l^* = l/l_c$, we obtain

$$P_2(l) = \frac{\pi^2}{4} \exp(-2\xi l^*) , \quad l^* \geq 1 , \tag{7}$$

$$P_2(l) = 4l^{*2}(1 - l^{*2})\, \xi^4 \left| \int_0^{\infty} \frac{x \exp(-x)\, dx}{(\xi^2 + x^2)^2 - 4l^{*2}\xi^2 x^2} \right| , \quad l^* < 1 , \tag{8}$$

and

$$Q_2 = \frac{2\pi}{k_i^2} \sum_{l=0}^{\infty} l\, P_2(l) .$$

The probability for the Coriolis mechanism is expo-

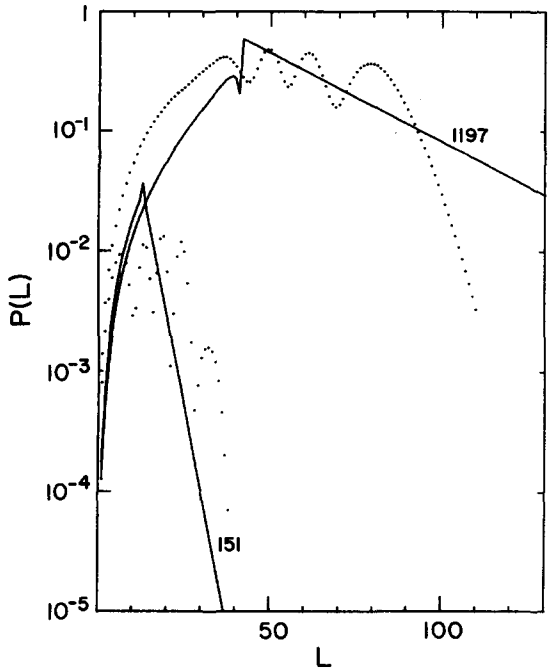

FIG. 9. $P(l)$ for the R_2 mechanism for K+He. Labeling as in Fig. 7. The 1197 and 151 K results are multiplied by 1.0.

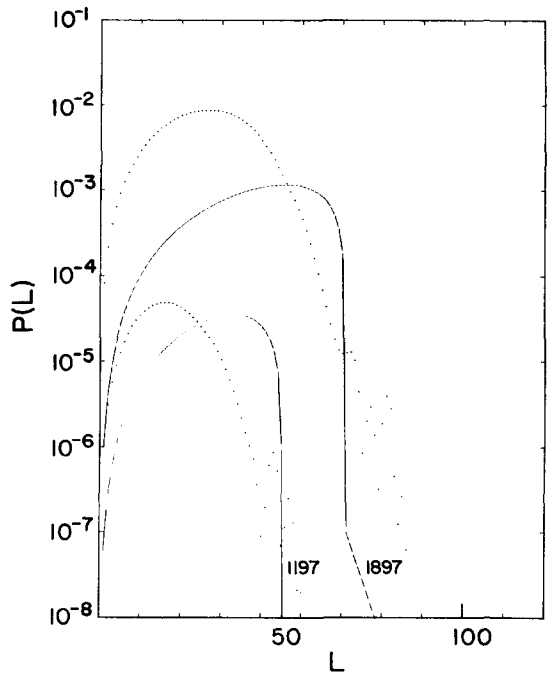

FIG. 11. As Fig. 9 but for Cs+He. The 1197 K results are multiplied by 1.0 and the 1897 K results are multiplied by 10.0.

nentially decreasing for large l. The integral can be efficiently evaluated (without calculating exponentials) by means of Laguerre integration.[35] This method works especially well for large ξ and l^* not too close to 1.

The comparison between the hard sphere Coriolis mechanism and the close coupled calculation is given in Figs. 6, 9, 10, and 11. The parameters ω and σ are given in Table I. We note the excellent agreement considering the crude model. The adiabatic perturbation theory result for P_2 is invalid for Na–He. Eq. (8) yields P_2 greater than unity for interesting energies for Na–He. Hence, we do not present $Q_{3/2}$ comparisons for this system.

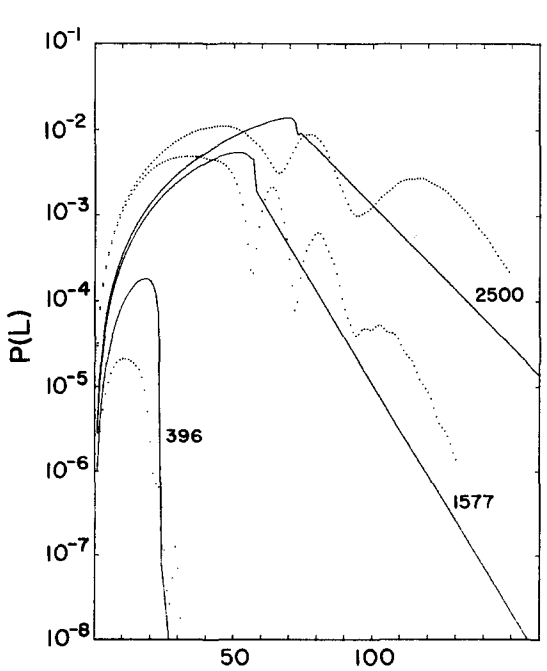

FIG. 10. As Fig. 9 but for Rb+He. The results for all energies are multiplied by 1.0.

VI. DISCUSSION

The results of this work can now be discussed and compared with other theoretical and experimental work. The quantum calculation presented here are reasonably simple to do, and they match experimental results well. The body fixed results are surprisingly well represented by the simple mechanisms for radial and angular mixing.

Our first conclusion is that the constant step size Magnus method is very effective in the integration of the coupled equations. Provided that the magic π instability is avoided, the partial cross sections are accurately calculated with a small number of intervals. If calculations are required only for low energies, entirely satisfactory results can be obtained with fewer intervals than we have used. The transformation matrices and the eigenvalues for each interval need to be calculated only once for use at all energies. Although we have used UNIX Fortran with eight byte arithmetic for these calculations, we estimate that all the integrations with 212 intervals for one energy require the equivalent of less than 4 s of CDC 7600 time.

The total cross sections for $^2P_{1/2} \rightarrow {}^2P_{3/2}$ intramultiplet mixing are presented in Figs. 3 and 4. The sodium results are very similar to the Reid and Dalgarno[8,9]

results that were obtained for the potentials of Baylis.[19] Figure 4 shows that the present results provide a reasonable fit to the experimental results of Anderson *et al.*[11] and Cuvellier *et al.*[12] The present quantum results also agree accurately with the PV potential calculation of Roueff and Launay.[36] The difference between the cross sections for the Baylis and PV potentials is also indicated. The agreement of the theoretical and experimental results shows that the total cross section measurements of Krause[2] for K($4p$)+He are about two times too large as has been noted by Olson.[17] The origin of this inconsistency should be resolved by redoing the thermal average results.

Figure 3 also shows the agreement of Gallagher's[10] $Q(v)$ results with the present calculation. The agreement is good for rubidium especially at the higher velocities. The rubidium results are similar to Olson's[17] Baylis[19] potential calculation. The agreement of the experiment and this work for Cs is only within an order of magnitude. The Olson cross sections have much better agreement with Gallagher's experiments. However the Reid–Dalgarno method is expected to be least appropriate for Cs+He collisions, because the PV potentials for Cs+He clearly show the effects of significant interaction of the $6p$ configuration with other configurations. The presence of such configuration interaction makes the Reid[9] procedure for obtaining V_0 and V_2 questionable. The experimental results are also more difficult to obtain for Cs than for Rb, because of the long wavelength of the emission and the very small fine structure state changing cross sections. Regardless of the source of the present disagreement with experiment, it is clear that the PV and Baylis potentials are quite different for Cs+He.

The calculations of this paper can easily give the intramultiplet mixing cross sections for polarized $^2P_{3/2}$ alkali atoms by using detailed balance on Eqs. (2b). Results for potassium are given in Fig. 5. The velocity dependence of transitions from $\Omega=\frac{1}{2}$ and $\Omega=\frac{3}{2}$ states are clearly very different. For $\Omega=\frac{1}{2}$ initial state the intramultiplet mixing must occur at low velocities by the radial mechanism, and for the $\Omega=\frac{3}{2}$ state mixing occurs by the angular mechanism. We see for this system that larger relative velocities are necessary to yield significant mixing by means of the angular mechanism. This is consistent with the analysis of Nikitin[5,6] which would predict that the radial (R_1) mechanism will be more important than the R_2 mechanism for low energy K+He collisions. We note however that the Ω conserving cross sections quickly reach their maximum value for $v=1.7$ km/s. Beyond this velocity the angular process has a larger cross section. Strictly speaking, the precise correspondence of the radial or angular mechanisms with the polarized atom cross sections is only valid for the low velocity region. This is because both angular and radial mechanisms can contribute to intramultiplet mixing of either Ω state. For example, angular coupling of a $\Omega=\frac{3}{2}$, $^2P_{3/2}$, initial state can produce $\Omega=\frac{1}{2}$ amplitude in the $^2P_{3/2}$ state during part of the collision. Radial coupling later in the collision can then convert this $\Omega=\frac{1}{2}$ amplitude into the $^2P_{1/2}$ state. The radial and angular mechanisms can only be used as first order interpretations in analyzing the results of a polarized atom experiment.

A better way to assess the relative importance of the first order radial or angular mechanisms is to compare the quantum results defined by Eqs. (2b) with simple semiclassical models. This is done in Fig. 6. This figure shows that the radial coupling model of Sec. IV and the angular coupling of Sec. V provide a very good approximation to the quantum results. The agreement is especially striking for K and for the $Q_{1/2}$ Rb results. The low velocity K and Rb $Q_{1/2}$ results show quantitative agreement between the exact and model calculations. The $Q_{3/2}$ agreement is less good for Rb and Cs. However, the highest energy Rb $Q_{3/2}$ cross sections have excellent agreement.

There is little doubt that the simple semiclassical models account nicely for the magnitude and the velocity dependence of the cross sections. Figure 6 shows that naive treatments for the nuclear motion can give excellent agreement with exact calculations. This figure shows the fundamental validity of Nikitin's ideas about intramultiplet mixing. Only simple estimates of the exchange interaction (α), the radial coupling radius (R_1), the $\Pi_{1/2}$, $\Pi_{3/2}$ separation (ω), and the angular coupling radius (σ) are necessary.

We have not presented radial mechanism results for Cs+He, because the PV potential has no radius where $V(\Sigma)-V(\Pi)=\Delta\epsilon$. Hence, it is not clear which R_1 or α should be used for this system. Certainly values for R_1 and α can be found that will reproduce the Cs $Q_{1/2}$ results, but the resulting agreement would only be data fitting and not a test of the simple model.

Since it is generally known that good agreement for total cross sections can be obtained with a poor model, we present a more detailed comparison of the quantum and model results in Figs. 7–11. These figures compare the transition probabilities calculated with Eqs. (2a) with the P_1 results of Eqs. (3) and (4) and the P_2 results of Eqs. (7). These comparisons of the transition probabilities for various orbital angular momenta provide important insight into the validity of the simple models.

Radial coupling results are presented for K+He in Fig. 7. We find excellent agreement at small l for the quantum calculations and the R_1 model. The model transition probabilities fall sharply at large l, because the simple model makes no allowance for tunneling. The model assumes that only collisions with impact parameters less than R_1 can contribute to intramultiplet mixing. The quantum results have probability at impact parameters greater than R_1. The other main difference in the quantum and model calculations is the presence of oscillations in the quantum results. These oscillations that arise from interference of the amplitudes in the various states are completely neglected in the simple radial coupling mechanism. Phase interference can be added to the semiclassical R_1 model, and then agreement with the oscillations should be found if the PV potentials are explicitly used in the model. However this would add considerable complexity to the model, and

would not show as nicely the basic physical importance of the R_1 mechanism.

Figure 8 shows the P_1 comparison for Rb+He. Here the agreement is not as satisfying, but the qualitative features of the quantum and model calculations are much like those in Fig. 7. The main difference for the 1577 Kayser result is the small and increasing quantum P for small l. The simple model greatly overestimates the transition probability in this angular momentum range.

Figure 9 presents P_2 comparisons for K+He. The simple hard sphere model does a good job of representing the quantum results. Both the quantum and model calculations have P that increases initially with increasing l. The l value at which tunneling is assumed is given by the l at which the straight lines begin. We see that the simple exponential treatment of tunneling is a good approximation to the average of the oscillating results. The feature in the model results at the angular momentum corresponding to $b=\sigma$ is only an artifact of the Laguerre integration used to evaluate P_2. The denominator in the second of Eqs. (7) has a pole at $l^*=1$, and the 15 point Laguerre integration is not able to accurately evaluate the integral for l^* very near 1.

Figure 10 gives the P_2 comparisons for Rb+He. Again we note the qualitative agreement for small l and the good agreement in the large l region. The 396 K result shows that the basic l dependence of the quantum calculation is well represented by the hard sphere model, but the magnitude of P is significantly overestimated by the simple model.

Figure 11 gives the P_2 results for Cs+He. For this system, we see the poorest quantitative agreement. This is not surprising from the $Q_{3/2}$ results in Fig. 6. We note however that the P_2 results are qualitatively the same as the quantum calculation. For both of the energies shown, the P fall sharply for $l>l_c$.

For all of the P_2 comparisons, except the lowest energy Rb+He system, the quantum P is always larger at small l than the hard sphere model results. The reason for this is that for a real potential that does not have an infinitely steep repulsive wall, low l collisions have a smaller turning point than larger l collisions. This smaller r_t produces a more rapid angular rotation rate for the interatomic axis, and hence a more efficient angular mixing of the Π states. A model that uses a more realistic repulsive potential should result in better agreement for small l values.

In general, we find satisfactory agreement with the simple mechanisms and the quantum results in the $P(l)$ comparisons. It is clearly valid to account for intramultiplet mixing in terms of radial and angular mechanisms. Also the results of Figs. 6–11 show that a first order analysis of polarized atom results in terms of radial or angular mechanisms is valid at least for the heavier alkali atoms.

We note that cross sections for polarized atoms can be obtained from a space fixed formulation of the scattering problem. This has been done by Reid,[9] Wilson, and Shimoni,[20] and Pascale and Perrin.[21] However, the use of the body fixed formulation makes the interpretation in terms of radial or angular coupling very transparent.

The results in Figs. 6–11 are obtained with the parameters in Table I. The R_1 values for K and Rb are obtained from the requirement that $V(\Sigma)-V(\Pi)=\Delta\epsilon$ and α is calculated from the PV potentials. Nikitin's estimate of α as $2(2I^*)^{1/2}$ is quite accurate for K and is used in the table. The parameters affect the P_1 calculations in two ways. The value for α determines the magnitude of P_1 and larger α give larger P_1. The value of R_1 determines the maximum value of l from which radial mixing can occur. Q_1 scales as R_1^2. The ω and σ values for the hard sphere Coriolis model are also given in Table I. The values for ω are determined from the difference between the PV $^2\Pi_{1/2}$ and $^2\Pi_{3/2}$ potentials. For K+He, this gives ω very near Nikitin's estimate of $2\Delta\epsilon/3$, but the Rb and Cs ω values differ from this estimate. The values for σ in Table I are somewhat arbitrary, but they are near the turning points for the PV potentials. If σ is changed, we have found that the magnitude of Q_2 varies only slightly, however the l value at which tunneling begins is sensitive to the choice of σ. The slope of the tunneling exponential decrease also depends on σ.

In several places in this paper, we have noted problems with the Cs calculations. First there is disagreement with Gallagher's experiments.[10] Second there is not a satisfactory determination of R_1, and there is poor agreement with the simple R_2 mechanism. Finally, our Cs–He results are much larger than those of Olson[17] who uses the Baylis[19] potentials in his calculations. These problems can be traced to the nature of the PV[24] potential that mixes in many configurations of the Cs atom in determining the potential. For such a potential the simple procedure of Reid to determine V_0 and V_2 may be inadequate. The values of V_0 and V_2 will not correctly reproduce the interactions of a $6p^2P$ Cs atom with helium. Since the Baylis[19] potential seems to treat Cs–He transitions well, the PV potentials are probably incorrect for this system.

We conclude this paper with the observation that quantum calculations of intramultiplet mixing are quite simple to do, and the process can be considered to occur because of radial and angular mixing mechanisms. The magnitude of the cross sections for the two mechanisms are comparable and both must be considered to accurately evaluate the cross sections. Although the quantum results can not be easily scaled like the simple semiclassical models, they easily provide reliable results for new systems.

ACKNOWLEDGMENTS

I wish to thank Dr. R. Düren, Professor H. Pauly, and the Max Planck Institute in Göttingen for their hospitality during the initial stages of this work.

[1] R. W. Wood, Philos. Mag. 27, 1018 (1914); R. W. Wood and F. L. Mohler, Phys. Rev. 11, 70 (1918).
[2] L. Krause, Appl. Opt. 5, 1375 (1966), and references therein.
[3] E. E. Nikitin, Opt. Spektrosk. 19, 91 (1965).
[4] J. Callaway and E. Bauer, Phys. Rev. A 1072, 140 (1965).

[5]E. E. Nikitin, J. Chem. Phys. **43**, 744 (1965).
[6]E. I. Dashevskaya, E. E. Nikitin, and A. I. Reznikov, J. Chem. Phys. **53**, 1175 (1970).
[7]E. E. Nikitin and A. I. Reznikov, J. Phys. B **13**, L57 (1980), and references cited therein.
[8]R. H. G. Reid and A. Dalgarno, Phys. Rev. Lett. **22**, 1029 (1969); Chem. Phys. Lett. **6**, 85 (1970).
[9]R. H. G. Reid, J. Phys. B **6**, 2018 (1973).
[10]A. Gallagher, Phys. Rev. **172**, 88 (1968).
[11]R. W. Anderson, T. P. Goddard, C. Parravano, and J. Warner, J. Chem. Phys. **64**, 4037 (1976).
[12]J. Cuvellier, J. Berlande, C. Benoit, M. Y. Perrin, J. M. Mestdagh, and J. De Mesmay, J. Phys. B **12**, L461 (1979).
[13]J. M. Mestdagh, J. Cuvellier, J. Berlande, A. Binet, and P. de Pujo, J. Phys. B **13**, 4589 (1980).
[14]W. D. Phillips, C. L. Glaser, and D. Kleppner, Phys. Rev. Lett. **38**, 1018 (1977).
[15]W. D. Phillips, J. A. Serri, D. J. Ely, D. E. Pritchard, K. R. Way, and J. L. Kinsey, Phys. Rev. Lett. **41**, 937 (1978).
[16]J. Apt and D. E. Pritchard, J. Phys. B **12**, 83 (1978).
[17]R. E. Olson, Chem. Phys. Lett. **33**, 250 (1975).
[18]J. Pascale and R. E. Olson, J. Chem. Phys. **64**, 3538 (1976).
[19]W. E. Baylis, J. Chem. Phys. **51**, 2665 (1969); JILA Report No. 100, University of Colorado, Boulder, Colorado, 22 September 1969.
[20]A. D. Wilson and Y. Shimoni, J. Phys. B **7**, 1543 (1974); **8**, 2393 (1975).
[21]J. Pascale and M-Y. Perrin, J. Phys. B **13**, 1839 (1980).
[22]R. H. G. Reid and R. F. Rankin, J. Phys. B **11**, 55 (1978).
[23]W. H. Miller and C. W. McCurdy, J. Chem. Phys. **69**, 5163 (1978); C. W. McCurdy, H. D. Meyer, and W. H. Miller, *ibid.* **70**, 3177 (1979).
[24]J. Pascale and J. Vandeplanque, J. Chem. Phys. **60**, 2278 (1974) and their "Numerical Results and Potential Curves" supplement.
[25]A. M. Arthurs and A. Dalgarno, Proc. R. Soc. London Ser. A **256**, 540 (1960).
[26]M. Jacob and G. C. Wick, Ann. Phys. (N.Y.) **7**, 404 (1959).
[27]M. S. Child, *Molecular Collision Theory* (Academic, London, 1974).
[28]D. M. Brink and G. R. Satchler, *Angular Momentum* (Publisher, Oxford, 1968).
[29]J. C. Light, in *Methods in Computational Physics*, edited by M. Rotenberg (Academic, New York, 1971), Vol. 10, p. 111.
[30]R. W. Anderson, J. Chem. Phys. (to be published).
[31]R. G. Gordon, in *Methods in Computational Physics*, edited by M. Rotenberg (Academic, New York, 1971), Vol. 10, p. p. 81.
[32]M. R. Mitchell and R. W. Anderson (unpublished).
[33]I. S. Gradshteyn and I. M. Ryshik, *Tables of Integrals, Series and Products* (Academic, New York, 1965).
[34]D. E. Pritchard, N. Smith, R. D. Driver, and T. A. Brunner, J. Chem. Phys. **70**, 2115 (1978); M. Wainger, I. Al-Agil, T. A. Brunner, A. W. Karp, N. Smith, and D. E. Pritchard, *ibid.* **71**, 1977 (1979).
[35]M. Abramowitz and I. A. Stegun, *Handbook of Mathematical Functions*, Natl. Bur. Stand. (U.S. GPO, Washington, D.C., 1964).
[36]E. Roueff and J. M. Launay, J. Phys. B **10**, L173 (1977).